Heat Transfer Optimization in Irregular Enclosures with Nano-Encapsulated Phase Change Materials: A Hybrid LB–FDM Numerical Analysis

Youness Ighris[1*], *Bilal el hadoui*[2], *Yassine Bouhouchi*[1], *Mohsine Qaffou*[1], *Meryem Maiss*[1], *Zakaria sadiki*[3], *Jamal Baliti*[1], *Mohamed Hssikou*[1], *Mourad Kaddiri*[4]

[1] Research team in Smart Electrical, Mechanical and Energy Systems (SEMES), Polydisciplinary Faculty, University of Sultan Moulay Slimane, Beni Mellal, Morrocco
[2] Rabat National School of Mines (ENSMR), BP: 753 Agdal-Rabat, Morocco
[3] Energy Research Center, Thermal and Energy Research Team (ERTE) ENSAM- Mohammed V University in Rabat, Morocco
[4] Laboratory of Intelligent Systems, Advanced Mechanics and Renewable Energy, Faculty of Sciences and Technologies, University of Sultan Moulay Slimane, Beni Mellal, Morocco

Abstract. This numerical study examines free convection heat transfer in an irregularly shaped cavity filled with a phase-change material nano-encapsulated in water mixture at a volume fraction of 3.5%. A hybrid computational approach integrating the lattice Boltzmann method for fluid dynamics with the finite difference scheme for heat transfer is utilized. The influences of the normalized fusion temperature θ_f, wall energy strength χ, wall thickness δ, and Rayleigh number Ra on flow structure, phase change behavior, and thermal performance are systematically analyzed. The results indicate that intermediate fusion temperatures ($\theta_f \approx$0.3-0.4) provide an optimal interaction between natural convection and latent heat absorption, leading to enhanced NEPCM melting and higher average Nusselt numbers. Increasing wall energy strength and wall thickness promotes more uniform melting and improves thermal regulation within the cavity. In addition, higher Rayleigh numbers intensify convective motion, accelerate phase change, and further enhance heat transfer. These findings highlight the effectiveness of NEPCM-based fluids for improving thermal management in natural convection systems.

1 Introduction

During recent decades, extensive numerical and experimental research has been devoted to evaluating the effectiveness of nanofluids in enhancing heat transfer [1]–[3]. Incorporating metallic or non-metallic nanoparticles into a conventional base fluid generally leads to a noticeable improvement in its thermal properties [4]–[6]. Reported results indicate that using

* Corresponding author: youness.ighris@usms.ac.ma

nanofluids containing 2 vol% CuO, 2.5 vol% Al_2O_3, 2 vol% Cu, and 2.5 vol% CNT dispersed in water can increase the heat exchange rate by approximately 17.3%, 22%, 31%, and 22%, respectively. For instance, Ighris et al. [7] performed a numerical analysis of free convection within an optimized cavity filled with a hybrid ferro-nanofluid, using a hybrid LBM–FDM scheme with experimentally based variable properties and magnetic field effects. Their results showed that the hybrid numerical approach significantly reduces computational cost compared with the conventional LBM approach, while the inclusion of hybrid nanoparticles improves the thermal and hydrodynamic performances by nearly 9% and 16%, respectively, depending on the Rayleigh number, heat source size, and magnetic field intensity and orientation. In this context, researchers continue to explore innovative strategies to enhance heat exchange efficiency. One of the promising approaches involves the use of nanofluids, particularly for applications where reducing energy consumption is crucial.

A recent advancement in this field is the development of nano-encapsulated phase change materials (NEPCMs), where each nanoparticle consists of a core made of phase change material. PCMs can absorb large amounts of thermal energy while undergoing only small temperature variations during melting and solidification. Materials such as paraffin or n-alkanes, for instance, are known for their excellent thermal energy storage capabilities [8], enabling them to store heat during phase transition. Because of these advantages, PCMs are increasingly used in multiple engineering and industrial domains, including storage units, industrial processes, photovoltaic/thermal devices, heat pipes, building thermal management, solar energy systems, and even biomedical applications. However, their relatively low thermal conductivity, especially in the case of n-alkanes requires large surface areas to achieve efficient heat storage. To address this limitation, encapsulation techniques have been introduced, where PCMs are enclosed within nanoscale shells to prevent leakage and improve overall heat exchange performance. Recently, natural convection has attracted significant interest because of its wide applicability in industrial operations, biomedical technologies, and numerous natural processes. Within this context, several studies have reported that incorporating NEPCM particles into the working fluid can significantly improve its thermal behavior, leading to enhanced convective heat transfer performance. In this context, Ghalambaz et al. [9] investigated free convection of NEPCM suspensions inside an tilted porous cavity, where the nano-shells encapsulate PCMs that absorb or release latent heat near the heated and cooled boundaries. Using a finite element formulation, they analyzed the effects of fusion point, Stefan number, and tilt angle of the cavity on the flow and temperature fields. Their results revealed that NEPCM addition consistently enhances heat transfer, with optimal performance observed at a nondimensional fusion point of 0.5 and an inclination angle of 42°, while lower Stefan numbers further promote thermal efficiency. Ghalambaz et al. [10] also analyzed the thermal behavior of NEPCM suspensions flowing over a vertical plate embedded in a porous medium. In their model, each NEPCM particle consists of a PCM core that absorbs latent heat when the surrounding fluid temperature exceeds the fusion point. Using a high-order boundary-value formulation solved via an adaptive finite difference method, they showed that NEPCM addition systematically enhances heat exchange. Their results further indicated that lowering the fusion temperature of the PCM core strengthens thermal performance, and that two distinct solution branches may appear under strong opposing flow conditions. El Glili et al. [11] carried out a numerical study on natural convection in a square cavity filled with an NEPCM suspension. Their findings indicated that NEPCM particles significantly enhance thermal transfer, especially when the heating and cooling walls are aligned vertically. Specifically, for $Ra=10^6$, a 5% concentration of NEPCM led to an increase of about 11.5% in the average Nusselt number, highlighting the important role of NEPCMs in improving both heat transfer and thermal storage performance. Sharifi et al. [12] developed a multi-fidelity modeling framework combining CFD, machine learning, and statistical regression to evaluate the effective thermal conductivity of NEPCMs under natural convection in a cylindrical annulus. Their results demonstrated that thermal performance depends strongly on Rayleigh number, melting strength, and the alignment of the melt front with the convective zone. The study highlighted the complex interplay between latent heat effects and flow structures, showing that NEPCMs can transition from convection-dominated to phase-change-buffered regimes, offering guidance for optimizing thermal systems. Faraji et al. [13] numerically analyzed the passive cooling of an electronic component using a nano-enhanced PCM (NEPCM) with hybrid Cu–Al_2O_3 nanoparticles. Their study showed that both the position of the component and the inclination of the heat sink significantly influence heat transfer and flow patterns. Optimal cooling was achieved with a rectangular heat sink, an inclination of 90°, and a component positioned at $\delta = 0.5$, ensuring safe operation and minimal temperature gradients.

This study focuses on optimizing heat transfer in a cavity filled with Nano-Encapsulated Phase Change Materials (NEPCM) using a well-localized heating source, aimed at enhancing melting efficiency and thermal distribution. To perform this study efficiently and accurately, a hybrid lattice Boltzmann method (LBM) approach is employed. This method allows reducing computational time while maintaining high accuracy in simulating complex flows and NEPCM phase-change effects within the cavity.

2 Mathematical formulation

2.1 Problem statement

The present computational analysis focuses on an irregularly shaped cavity filled with a water-based NEPCM suspension. The flow regime is considered laminar, steady-state, and incompressible, with buoyancy effects modeled through the Boussinesq approximation. A partial heat source is mounted at the bottom-left corner of the enclosure and positioned to optimize heat transfer characteristics. Its dimension is adjusted using a specified size ratio parameter. The right-side vertical wall is maintained under isothermal cold conditions, while all other walls, including the horizontal boundaries, are assumed adiabatic. The cavity is considered sufficiently extended in the z-direction so that variations along this axis can be neglected. Therefore, the problem is modeled using a two-dimensional formulation in the (x, y) plane (see Fig. 1).

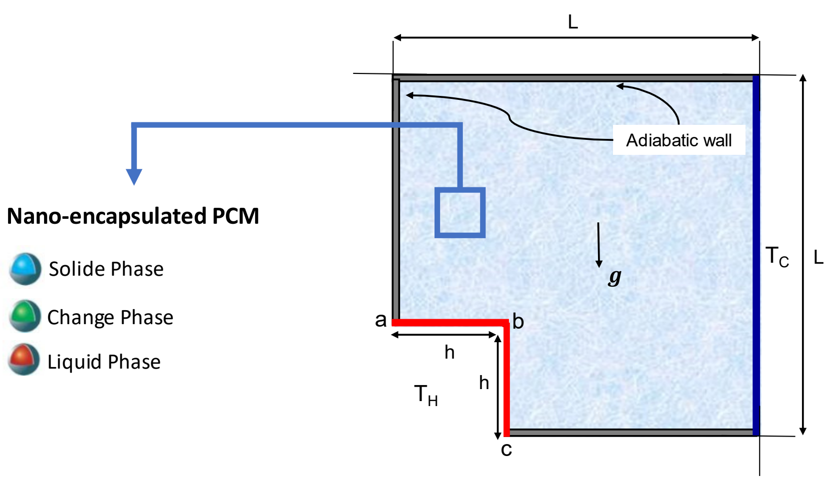

Fig. 1. Geometric configuration.

2.2 Governing equations

In this work, the flow of a NEPCM–water mixture is modeled under steady, two-dimensional, incompressible, and homogeneous conditions. Temperature-dependent variations in density are incorporated using the Boussinesq approximation to account for buoyancy effects. Accordingly, the governing momentum and energy equations are expressed as follows [12]:

$$\boldsymbol{\nabla}.\boldsymbol{v} = 0 \tag{1}$$

$$\rho \boldsymbol{v}.\boldsymbol{\nabla v} = -\boldsymbol{\nabla} p + \boldsymbol{\nabla}.(\mu \boldsymbol{\nabla v}) + \rho\beta\left(T - T_{ref}\right)\boldsymbol{g} \tag{2}$$

$$\boldsymbol{v}.\boldsymbol{\nabla}\left(\rho c_p T\right) = \boldsymbol{\nabla}.(k\boldsymbol{\nabla} T) \tag{3}$$

Here, the symbols ρ, μ, β, c_p, k, $\boldsymbol{g}$, $\boldsymbol{v}$, p, T, and T_{ref} denote, respectively, the mixture density, dynamic viscosity, thermal expansion coefficient, specific heat capacity, thermal conductivity, gravitational acceleration, velocity field, pressure, temperature, and reference temperature. Tensor quantities are indicated using bold notation.

2.3 NEPCM properties

According to Ref. [14], the phase-change behavior of the NEPCM core material (n-nonadecane) is characterized by melting and solidification temperatures of 32.12 °C and 31.9 °C, respectively. When the core is encapsulated within a polyurethane shell with a core-to-shell mass ratio of 0.447, these temperatures shift to 30.54 °C for melting and 30.78 °C for solidification. It should be noted that the overall thermophysical properties of NEPCMs result from the combined contributions of both the core and shell materials, as discussed in Ref. [15].

$$\rho_n = \frac{(1 + m_r)\rho_c\rho_s}{m_r\rho_c + \rho_s}. \tag{4}$$

Here, ρ denotes the density, while the subscripts c, s, and n refer to the core, shell, and NEPCM, respectively. The parameter m_r represents the core-to-shell mass ratio, defined as $m_r = \frac{m_{core}}{m_{shell}}$.

The specific heat capacity of the core material is assumed to be constant at the pure melting and solidification temperatures and is denoted by $c_{p,cl}$. However, within the phase-change interval where latent heat effects are taken into account, the core specific heat capacity $c_{p,c}$ is modeled using the sinusoidal formulation described as follows:

$$c_{p,c} = \begin{cases} 0 & ;\text{if } T < T_f - \frac{T_{mr}}{2} \\ c_{p,cl} + \left\{\frac{\pi}{2}\left(\frac{L_f}{T_{mr}} - c_{p,cl}\right)\left(sin\pi\frac{T - (T_f - \frac{T_{mr}}{2})}{T_{mr}}\right)\right\}; & \text{if } T_f - \frac{T_{mr}}{2} < T < T_f + \frac{T_{mr}}{2} \\ 0 & ;\text{if } T < T_f + \frac{T_{mr}}{2} \end{cases} \tag{5}$$

The specific heat capacity of the NEPCM ($c_{p,n}$), which results from the combined contributions of the core and shell materials, is expressed as follows[15]:

$$c_{p,n} = \frac{(c_{p,c} + m_r c_{p,s})\rho_c \rho_s}{(m_r \rho_c + \rho_s)\rho_n}. \quad (6)$$

The effective thermal expansion coefficient of a spherical particle composed of dissimilar core and shell materials can be expressed as follows [15]:

$$\beta_n = \beta_c + \left(\frac{\beta_s - \beta_c}{2}\right)\left(1 - m_r \frac{\rho_s}{\rho_c}\right). \quad (7)$$

2.4 Mixture properties

The density, specific heat capacity, and thermal expansion coefficient of the present mixture are evaluated using the following relations [12]:

$$\rho_m = (1 - \varphi)\rho_f + \varphi \rho_n, \quad (8)$$

$$c_{p,m} = \frac{(1 - \varphi)\rho_f c_{p,f} + \varphi \rho_n c_{p,n}}{\rho_m}, \quad (9)$$

$$\beta_m = \frac{(1 - \varphi)\rho_f \beta_f + \varphi \rho_n \beta_n}{\rho_m}. \quad (10)$$

In the above equations, φ denotes the NEPCM volume fraction, while the subscript m refers to the mixture properties.

The thermal conductivity and dynamic viscosity of water-based NEPCM suspensions with a core–shell mass ratio of 0.447 (n-nonadecane core and polyurethane shell) were determined experimentally. A fifth-order polynomial correlation is employed to model the thermal conductivity ratio as follows [14]:

$$k_m / k_f = (1 - 0.3925\varphi + 0.7141\varphi^2 - 0.4177\varphi^3 + 0.1055\varphi^4 - 0.0098\varphi^5). \quad (11)$$

The viscosity of the mixture is evaluated using the following correlation [14]:

$$\mu_m / \mu_f = (1 + 0.125\varphi + 0.0006\varphi^2). \quad (12)$$

Table 1 summarizes the thermophysical properties of water, n-nonadecane, and polyurethane at 303 K, based on the data provided in Ref. [14].

Table 1. Thermophysical properties of water, n-nonadecane (core), and polyurethane (shell) in 305K.

	$\rho\ (\frac{kg}{m^3})$	$c_p\ (\frac{J}{kg.K})$	$10^5\beta\ (\frac{1}{K})$	$10^2 k\ (\frac{W}{m.K})$	$10^5\mu(Pa.s)$
base fluid	995.7	4178	36.6	62.3	72.4
core	721	2037	50	19	_
shell	786	1317	17.3	2.5	_

3 Numerical simulation

In this study, a numerical model was developed to investigate natural convection in an irregular cavity filled with a water–NEPCM mixture. The model employs a hybrid approach, combining the lattice Boltzmann method (LBM) for the momentum equations and the finite difference method (FDM) for the energy equation, implemented in FORTRAN. The NEPCM volume fraction was fixed at φ=3.5%, and different Rayleigh numbers Ra=10^4 and Ra=10^5. A uniform grid of 240×240 was used for all simulations to ensure accuracy and convergence of the results.

Several dimensionless parameters were introduced to characterize the phase-change behavior and wall energy effects:

θ_f: the normalized fusion (phase-change) temperature of the NEPCM;

δ : the thickness of the energy wall;

χ : the wall energy strength.

For the simulations, the parameters were set as 0.1<θ_f<0.9 for δ = 0.2 and δ = 0.5 with χ=20, 50, 100.

3.1 Results and discussion

Figures 2 present the variation of the average Nusselt number ($\overline{\text{Nu}}$) as a function of the normalized fusion temperature (θ_f) for two Rayleigh numbers, Ra = 10^4 and Ra = 10^5, considering two energy wall thicknesses (δ = 0.2 and δ = 0.5) and different wall energy strengths (χ = 20, 50, and 100).

At Ra = 10^4, the average Nusselt number exhibits a non-monotonic evolution with respect to θ_f for all investigated values of δ and χ. As θ_f increases, $\overline{\text{Nu}}$ initially rises, reaches a maximum at an intermediate fusion temperature ($\theta_f \approx$ 0.3–0.4), and then decreases for higher θ_f values. This behavior is attributed to the timing of the NEPCM phase change. At low fusion temperatures, the phase change occurs early, leading to premature latent heat absorption and reduced temperature gradients near the heated wall. At intermediate θ_f, the phase change coincides with a well-developed thermal field, resulting in an optimal interaction between latent heat storage and buoyancy-driven convection, and consequently maximizing the heat transfer rate. At higher θ_f, the delayed phase change weakens the contribution of latent heat during the main convective regime, causing a reduction in $\overline{\text{Nu}}$. For a fixed θ_f, increasing the wall energy strength χ enhances $\overline{\text{Nu}}$, while a larger wall thickness (δ = 0.5) consistently yields higher heat transfer rates compared to δ = 0.2. These trends indicate that wall thermal energy storage plays a positive role in regulating the heat transfer process under moderate convection conditions. When the Rayleigh number increases to Ra = 10^5, the same qualitative trends are observed, but with significantly higher values of the average Nusselt number. This increase reflects the dominance of stronger buoyancy-driven convection, which intensifies fluid motion and enhances thermal mixing within the cavity. However, the enhancement associated with increasing χ becomes more pronounced at Ra = 10^5, indicating that stronger wall–fluid thermal interaction is particularly effective when convection is dominant. Moreover, the influence of the energy wall thickness is amplified at higher Ra. The thicker energy wall (δ = 0.5) provides greater thermal capacity, allowing more efficient energy exchange between the wall and the fluid–NEPCM mixture, which leads to a further increase in heat transfer performance.

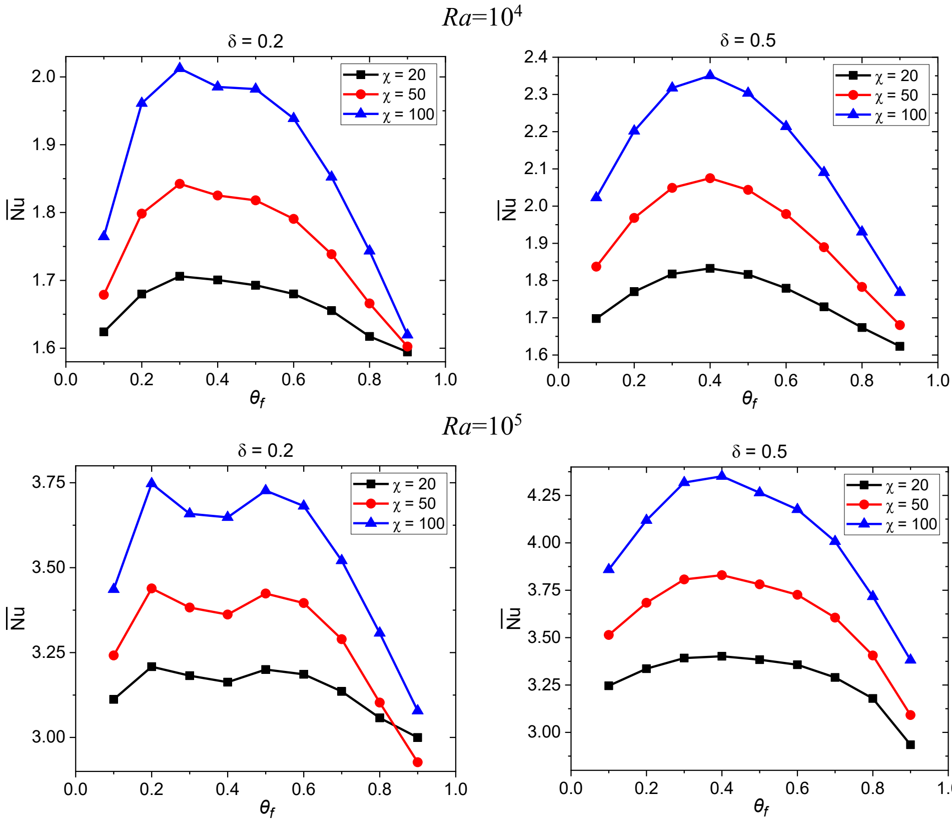

Fig. 2. Variation of the average Nusselt number ($\overline{\mathrm{Nu}}$) as a function of the normalized fusion temperature (θ_f) for two Rayleigh numbers ($Ra = 10^4$ and $Ra = 10^5$), considering two energy wall thicknesses (δ = 0.2 and δ = 0.5) and different wall energy strengths (χ = 20, 50, and 100).

Figures 3 illustrate the contours of the heat capacity ratio Cr at $Ra = 10^4$ for two wall energy strengths, χ = 20 and χ = 100, considering two energy wall thicknesses (δ = 0.2 and δ = 0.5) and three normalized fusion temperatures, θ_f = 0.1, 0.4, and 0.9. For all configurations, the distribution of Cr is strongly influenced by the fusion temperature. At low melting temperatures (θ_f = 0.1), high Cr values are concentrated near the cold right wall. This indicates that NEPCM begins to melt primarily in areas where heat accumulation is delayed, resulting in limited heat transfer and a less uniform thermal distribution within the cavity. At intermediate fusion temperature (θ_f = 0.4), the Cr contours become more spatially distributed and better aligned with the convective flow structure. The melting process occurs when the thermal field is already developed, leading to a more effective interaction between phase change and natural convection. This configuration corresponds to the optimal thermal performance observed in the Nusselt number results. At high fusion temperature (θ_f = 0.9), the Cr contours show limited melting regions confined close to the heated wall. The delayed phase change reduces the contribution of latent heat storage during the main convective regime, resulting in weaker thermal regulation and reduced heat transfer enhancement. Influence of wall energy strength χ Comparing χ = 20 and χ = 100, it is evident that increasing the wall energy strength significantly intensifies the Cr field. For χ = 100, higher Cr values occupy a larger portion of the cavity, indicating a stronger and more uniform phase-change process. This behavior reflects enhanced energy exchange between the wall and the fluid–NEPCM mixture, which promotes melting and improves thermal distribution. In contrast, for χ = 20, the melting regions are more localized and less intense, especially at high θ_f, confirming that weaker wall–fluid thermal interaction limits the effectiveness of the phase-change mechanism. Effect of energy wall thickness δ for both χ values, increasing the wall thickness from δ = 0.2 to δ = 0.5 leads to a noticeable expansion of the melting zones. The thicker energy wall provides greater thermal capacity, allowing more energy to be stored and gradually released to the NEPCM. This results in higher Cr values and smoother spatial gradients, particularly at intermediate fusion temperatures. The combined effect of δ = 0.5 and χ = 100 produces the most favorable Cr distribution, characterized by extended melting regions and enhanced thermal uniformity within the cavity. Physical consistency and link with heat transfer results. The Cr contour analysis is fully consistent with the Nusselt number trends observed for Ra = 10^4. Early melting at low θ_f explains the limited heat transfer enhancement. Optimized melting patterns at intermediate θ_f justify the maximum $\overline{\mathrm{Nu}}$ values. Delayed melting at high θ_f leads to reduced thermal performance. Overall, the Cr contours confirm that the timing and spatial distribution of the NEPCM phase change, controlled by θ_f, χ, and δ, play a crucial role in regulating heat transfer under moderate natural convection conditions.

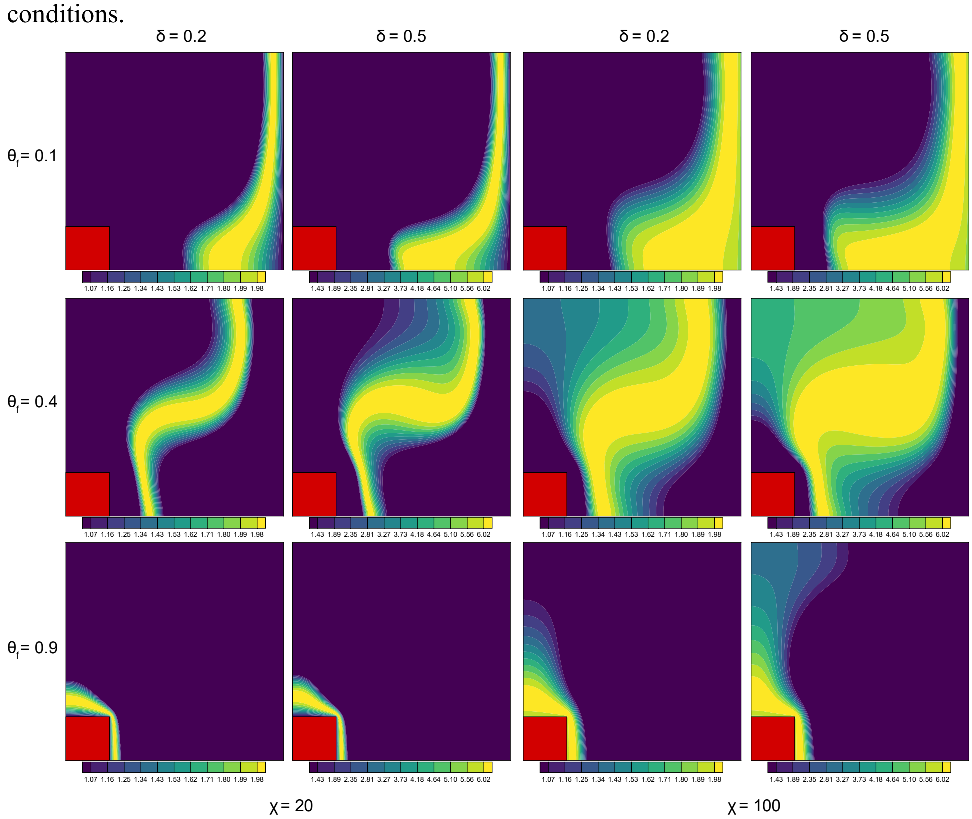

Fig. 3. Contours of Cr at Ra = 10^4 for χ = 20 and χ = 100, with wall thicknesses δ = 0.2 and 0.5, fusion temperatures θ_f = 0.1, 0.4, 0.9, and NEPCM volume fraction φ = 3.5%.

Conclusion

Natural convection in complex-shaped cavities containing NEPCM with a volume concentration of φ =3.5% was numerically investigated in this work. The study evaluated the impacts of fusion temperature, wall energy parameter, wall thickness, and Rayleigh number on thermal behavior and heat transfer performance.

The main findings are:

- Effect of θ_f: low fusion temperatures concentrate high Cr near the cold wall, delaying effective latent heat absorption, while intermediate θ_f promotes optimal interaction between phase change and natural convection, maximizing thermal performance and average Nusselt number ($\overline{Nu}$). High θ_f delays melting and reduces heat transfer enhancement.
- Effect of wall properties (χ and δ): increasing wall strength and thickness extends melting regions, promotes uniform Cr distribution, and enhances thermal regulation, resulting in higher $\overline{Nu}$.
- Effect of *Ra*: higher *Ra* intensifies convection, alters flow structure, and accelerates NEPCM melting, improving heat transfer.

Overall, NEPCM proves to be a promising solution for thermal management in natural convection systems, with wall properties and phase-change parameters playing a key role in achieving optimal heat transfer performance.

References

[1] K. Thirumalaisamy and S. Ramachandran, "Comparative heat transfer analysis on Fe3O4–H2O and Fe3O4–Cu–H2O flow inside a tilted square porous cavity with shape effects," *Phys. Fluids*, vol. 35, no. 2, Feb. 2023, doi: 10.1063/5.0136326.

[2] Y. Ighris, Y. Bouhouchi, Y. Elguennouni, J. Baliti, M. Hssikou, and A. Boumezzough, "Numerical study of natural convection in an inclined cavity filled with Al2O3/Cu-H2O nanofluids," *Numer. Heat Transf. Part A Appl.*, vol. 0, no. 0, pp. 1–25, 2024, doi: 10.1080/10407782.2024.2314230.

[3] Y. Ighris, B. El hadoui, J. Baliti, Y. Elguennouni, and M. Hssikou, "Optimizing thermal management of convective heat transfer in a complex nanofluid-filled cavity using the lattice Boltzmann method," *Int. J. Numer. Methods Heat Fluid Flow*, vol. 35, no. 5, pp. 1845–1883, Jun. 2025, doi: 10.1108/HFF-01-2025-0044.

[4] Y. Hu, Y. He, C. Qi, B. Jiang, and H. Inaki Schlaberg, "Experimental and numerical study of natural convection in a square enclosure filled with nanofluid," *Int. J. Heat Mass Transf.*, vol. 78, pp. 380–392, Nov. 2014, doi: 10.1016/j.ijheatmasstransfer.2014.07.001.

[5] B. El Hadoui, Y. Ighris, M. Kaddiri, and J. Baliti, "Thermal management and heat transfer enhancement through heatlines visualization in a moving-wall chamber: effects of shear, heater geometry, and nanoparticle suspension," *Int. J. Therm. Sci.*, vol. 217, p. 110098, Nov. 2025, doi: 10.1016/j.ijthermalsci.2025.110098.

[6] Y. Ighris *et al.*, "Thermal management optimization of natural convection in a triangular chamber: Role of heating positions and ternary hybrid nanofluid," *Phys. Fluids*, vol. 36, no. 9, Sep. 2024, doi: 10.1063/5.0226427.

[7] Y. Ighris, B. El, M. Qaffou, and J. Baliti, "International Journal of Thermal Sciences Hybrid lattice Boltzmann modeling of magneto-convection in Fe 2 O 3 / MWCNT ferro-nanofluid for thermal management applications," *Int. J. Therm. Sci.*, vol. 220, no. PB, p. 110433, 2026, doi: 10.1016/j.ijthermalsci.2025.110433.

[8] A. Sarı, C. Alkan, A. Biçer, and C. Bilgin, "Micro / nanoencapsulated n - nonadecane with poly (methyl methacrylate) shell for thermal energy storage," vol. 86, pp. 614–621, 2014, doi: 10.1016/j.enconman.2014.05.092.

[9] M. Ghalambaz, S. A. M. Mehryan, I. Zahmatkesh, and A. Chamkha, "International Journal of Thermal Sciences Free convection heat transfer analysis of a suspension of nano – encapsulated phase change materials (NEPCMs) in an inclined porous cavity," *Int. J. Therm. Sci.*, vol. 157, no. June, p. 106503, 2020, doi: 10.1016/j.ijthermalsci.2020.106503.

[10] M. Ghalambaz, T. Gro, and I. Pop, "Mixed convection boundary layer fl ow and heat transfer over a vertical plate embedded in a porous medium fi lled with a suspension of nano-encapsulated phase change materials," *J. Mol. Liq.*, vol. 293, p. 111432, 2019, doi: 10.1016/j.molliq.2019.111432.

[11] I. El, G. Youness, F. Hafsa, A. Mohamed, and S. Mohamed, "Natural convection enhancement with nano - encapsulated phase change materials in differentially heated square cavities," *J. Therm. Anal. Calorim.*, no. 0123456789, 2025, doi: 10.1007/s10973-025-15102-x.

[12] M. Sharifi *et al.*, "Statistical and machine learning approaches integrated with CFD for effective thermal conductivity prediction of NEPCMs in natural convection between horizontal concentric cylinders," *J. Energy Storage*, vol. 141, no. PC, p. 119340, 2026, doi: 10.1016/j.est.2025.119340.

[13] H. Faraji, M. El Alami, A. Arshad, and Y. Hariti, "Numerical survey on performance of hybrid NePCM for cooling of electronics: Effect of heat source position and heat sink inclination," *J. Therm. Sci. Eng. Appl.*, vol. 13, no. 5, 2020, doi: 10.1115/1.4049431.

[14] Z. Qiu and L. Li, "Experimental and numerical investigation of laminar heat transfer of microencapsulated phase change material slurry (MPCMS) in a circular tube with constant heat flux," *Sustain. Cities Soc.*, vol. 52, no. August 2019, p. 101786, 2020, doi: 10.1016/j.scs.2019.101786.

[15] E. Golab, S. Goudarzi, H. Kazemi-varnamkhasti, and H. Amigh, "Investigation of the effect of adding nano-encapsulated phase change material to water in natural convection inside a rectangular cavity," vol. 40, no. April, 2021.